Phyton-
International Journal of
Experimental Botany

Tech Science Press

http://doi.org/10.32604/phyton.2026.075656

ARTICLE

Moderate CO_2 Enrichment Enhances Saponin Accumulation in *Panax japonicus* by Activating Sugar Metabolism

Xiao Wang*, E Liang, Xiaohui Song and Deyan Li

College of Agriculture, Anshun University, Anshun, China
*Corresponding Author: Xiao Wang. Email: hopewangxiao@163.com

Received: 05 November 2025; Accepted: 29 December 2025; Published: 31 March 2026

ABSTRACT: Three-year-old *Panax japonicus* was exposed to elevated CO_2 concentrations using open-top chambers: ambient CO_2 (aCO_2), moderately elevated ($e1CO_2$, 550 μmol/mol), and highly elevated ($e2CO_2$, 750 μmol/mol). Gas exchange parameters, photosynthetic pigments, sugar accumulation, and total saponin content were measured to assess the effects of CO_2 enrichment on photosynthesis, sugar metabolism, and saponin biosynthesis. The $e1CO_2$ treatment significantly increased net photosynthetic rate (by 17.22% at 36 days and 69.62% at 92 days), chlorophyll a content, and soluble sugar, sucrose, and starch accumulation. Key sugar metabolism enzymes, including sucrose phosphate synthase (SPS), also showed enhanced activity. Consequently, underground rhizome total saponins rose significantly by 15.16%. In contrast, $e2CO_2$ initially (36 days) stimulated photosynthesis but lost this effect over prolonged exposure (92 days), with no significant impact on photosynthetic parameters, pigments, or sugar levels. Correlation analysis indicated that rhizome saponin content was positively associated with leaf sucrose levels and sucrose synthase (synthetic direction) activity. These findings suggest that moderate CO_2 elevation ($e1CO_2$) enhances *P. japonicus* photosynthesis and sugar metabolism, driving greater saponin accumulation. However, high CO_2 ($e2CO_2$) has transient benefits, with stimulatory effects diminishing over time.

KEYWORDS: *Panax japonicus*; elevated CO_2 concentration; photosynthetic characteristics; sugar metabolism; saponin accumulation

1 Introduction

Anthropogenic activities have elevated atmospheric carbon dioxide (CO_2) concentrations from a pre-industrial level of approximately 280 ppm to over 420 ppm today and are a primary driver of global climate change [1]. Beyond its climatic effects, this CO_2 enrichment (eCO_2) acts as a fundamental "aerial fertilizer" for plant growth. Meta-analyses of Free-Air CO_2 Enrichment (FACE) studies provide robust statistical evidence of this fertilization effect: for instance, eCO_2 at concentrations ranging from 500–600 ppm can stimulate the yield of major C_3 cereal crops like wheat and rice by 10–25% and root crops by 25–38% under optimal conditions [2]. This yield enhancement is directly linked to the core physiological impact of eCO_2 on C_3 plants: the competitive inhibition of ribulose-1,5-bisphosphate carboxylase/oxygenase oxygenation, which reduces photorespiration and thereby increases net CO_2 assimilation rates. In FACE studies, photosynthesis in C_3 species typically increases by 20–40% under these conditions [3]. This global phenomenon extends beyond staple food crops to medicinal plants, where increased photosynthetic carbon fixation can cascade into secondary metabolism by altering the availability of carbon precursors and energy supply. Numerous studies have investigated the effects of eCO_2 on the growth and secondary metabolism of

medicinal plants, such as *Polygonatum kingianum* [4], *Typha orientalis* [5], *Lycium barbarum* [6], *Dendrobium officinale* [7], *Mentha piperita* [8], and *Paris polyphylla* [9]. *Panax japonicus* C. A. Meyer, a perennial herbaceous plant, is one of China's rare and endangered medicinal herbs and is locally regarded as the "King of Herbal Medicines". Its primary bioactive constituents include saponins, carbohydrates, and amino acids [10]. As a typical C3 plant, *P. japonicus* exhibits high photosynthetic responsiveness to eCO_2. More importantly, it possesses a robust underground rhizome sink that serves as the primary site for the translocation and storage of photoassimilates like sucrose, establishing a direct source-sink pathway from leaf photosynthesis, where sucrose functions not only as a critical carbon skeleton but also as an energy substrate for the biosynthesis of secondary metabolites, including saponins. While most existing studies on *P. japonicus* have focused on its chemical composition [11], pharmacological activity [12], quality evaluation [13], and gene regulation [14], physiological and ecological research related to cultivation remains limited. Given these physiological traits, *P. japonicus* is a well-suited candidate for uncovering the cascade of events from eCO_2-induced carbon assimilation and allocation through sugar metabolic pathways to the eventual partitioning of carbon into saponin production.

Saponin accumulation in the underground organs of medicinal plants such as *P. japonicus* is fundamentally governed by carbohydrate availability and translocation from aerial tissues [15]. Following photosynthetic CO_2 assimilation, sucrose serves as the primary transport form of photoassimilates and is partitioned into underground organs, where it is metabolized by key enzymes–including sucrose synthase (SS), sucrose phosphate synthase (SPS), and neutral invertase (NI)–to generate soluble sugars that fuel secondary metabolic pathways such as saponin biosynthesis [16,17]. The glycosylation of aglycones, an essential step in saponin formation, is intrinsically dependent on carbohydrate supply, with uridine diphosphate glucose (UDPG)–derived from sucrose metabolism–serving as the key glycosyl donor for triterpenoid skeletons [18,19]. In underground tissues, the substrate for UDPG synthesis is primarily supplied by leaf photosynthesis, and its abundance is governed by photosynthetic intensity and the translocation efficiency of sucrose [20,21]. Thus, saponin accumulation in below-ground organs is closely linked to photosynthetic activity, sugar metabolism, and carbohydrate status in above-ground parts [22]. While eCO_2 has been shown to enhance sugar accumulation and related enzyme activities, its effect on final saponin content is often species-specific and dependent on exposure duration [23,24]. These physiological and biochemical mechanisms provide a theoretical basis for the hypothesis that eCO_2 may influence medicinal plant quality by modulating carbon allocation from source leaves to sink organs.

This study investigated the effects of eCO_2 on photosynthesis, sugar metabolism, and saponin accumulation in *P. japonicus*. We hypothesized that a moderate CO_2 elevation ($e1CO_2$, 550 μmol/mol) would sustainably enhance the net photosynthetic rate, upregulate the activity of key sugar-metabolizing enzymes, and consequently promote carbon allocation towards sucrose and total saponin biosynthesis in the rhizome. In contrast, a higher CO_2 level ($e2CO_2$, 750 μmol/mol) was anticipated to induce only a transient photosynthetic enhancement, with acclimation effects (CO_2 level × exposure time interaction) diminishing its long-term benefits on carbon assimilation and partitioning into secondary metabolites. By integrating these physiological and metabolic responses, this study aims to elucidate the mechanistic basis of how eCO_2 modulates the carbon flux from primary photosynthesis to secondary saponin biosynthesis in *P. japonicus*, thereby providing theoretical insights into the impact of future climatic changes on the quality of medicinal plants.

2 Materials and Methods

2.1 Plant Material and Substrate

The plant material used in this study was *P. japonicus* rhizomes. These rhizomes were sourced in November 2024 from a commercial nursery located in Banqiao Town, Enshi City, Enshi Tujia and Miao Autonomous Prefecture, Hubei Province, China, where they had been grown for three years under standardized cultivation practices. The pre-experimental growth conditions at the nursery involved cultivation under a natural forest canopy, providing approximately 60–70% shade. The plants experienced natural ambient temperature and precipitation cycles with supplemental drip irrigation applied during extended dry periods. In November 2024, uniformly sized, three-year-old rhizomes were transplanted into nine cultivation frames (three frames per open-top chamber) with each frame measuring 111 cm × 37 cm × 34 cm. The three OTCs corresponded to three CO_2 treatments: ambient CO_2 (aCO_2), and two elevated CO_2 levels ($e1CO_2$ and $e2CO_2$). Each frame contained 20 rhizomes, and frames were randomly positioned within each chamber to avoid positional effects. The plants were allowed to establish and overwinter in the OTCs under ambient conditions. The cultivation substrate consisted of a mixture of yellow soil, nutrient soil, vermiculite, and pig manure compost, with the following nutrient composition: pH 6.7; available nitrogen 38.4 mg/kg; available phosphorus 18.9 mg/kg; available potassium 148.8 mg/kg; organic matter 6.3%.

The experimental apparatus comprised octagonal OTCs, each with eight sides, a side length of 1.0 m, a height of 1.7 m, and a top inclined 45° inward (Fig. 1).

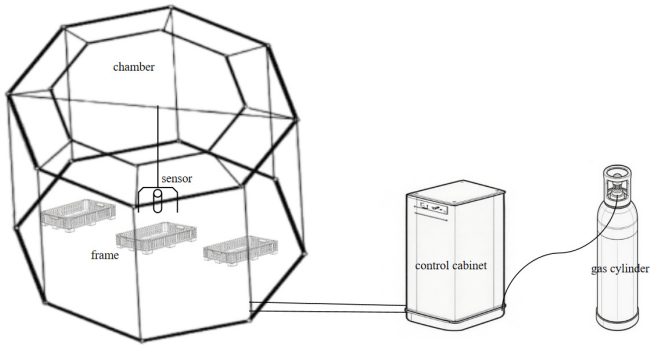

Figure 1: The open-top chamber CO_2 concentration control system.

2.2 Methods

2.2.1 Experimental Method

The experiment was conducted with three CO_2 concentration treatments: aCO_2, $e1CO_2$ and $e2CO_2$. The aCO_2 treatment served as the control, with no additional CO_2 introduced into the chambers. In contrast, CO_2 gas was supplied to the $e1CO_2$ and $e2CO_2$ chambers. The microclimatic conditions within the OTCs were closely monitored and controlled. The CO_2 concentration was regulated using a sensor (GMP-220, Vaisala, Finland) positioned 20 cm above the mean plant canopy height and connected to a data logger. This system transmitted real-time data to a control computer, which executed a programmed feedback mechanism to operate electromagnetic valves, thereby maintaining the CO_2 concentrations within the specified targets. In addition to CO_2, air temperature and relative humidity were continuously monitored at a height of 20 cm above the mean plant canopy height inside each chamber using integrated sensors (MTK-TH800, Asmik, Guangzhou, China), with data logged at 10-min intervals. The continuous time-series data for all parameters were recorded to verify the stability and accuracy of the treatment conditions throughout

the experiment. Specifically, the CO_2 concentrations were maintained at 550 μmol/mol for the e1CO_2 treatment and 750 μmol/mol for the e2CO_2 treatment. These setpoints were selected to simulate projected atmospheric CO_2 levels, corresponding to mid-century and end-of-century projections, respectively, under the intermediate SSP2-4.5 scenario as outlined in the IPCC Sixth Assessment Report [25]. This approach is widely used to assess plant responses to future climate conditions. Continuous monitoring data of CO_2 concentrations in each chamber during the entire experimental period demonstrate that CO_2 levels were maintained at stable mean values of 548.6 ± 9.3 μmol/mol for the e1CO_2 treatment and 747.1 ± 8.7 μmol/mol for the e2CO_2 treatment, confirming effective control around the target setpoints. Each CO_2 treatment consisted of three frames with each frame consisting of 20 seedlings. The elevated CO_2 treatments commenced on April 11, 2025, shortly after the spring sprouting. Throughout the experimental period, soil moisture was maintained by timely and equal-volume watering to keep the soil consistently moist. Weeds were regularly removed by hand to minimize competition. To assess any potential microclimatic modification by the chambers, air temperature was measured both inside each OTC at canopy height and at corresponding heights in adjacent open-field plots. Air temperature varied naturally across the study period. The ambient temperature ranged from a minimum of 6°C to a maximum of 30°C. Inside the chambers, temperatures closely tracked these external conditions, with a mean chamber effect (temperature difference, inside minus outside) of +0.3°C, confirming minimal thermal alteration by the OTCs. Relative humidity in the ambient environment ranged between 75% and 84%. Gas exchange parameters of *P. japonicus* leaves were measured at 36 days (leaf expansion stage) and 92 days (nutrient accumulation stage) after the initiation of CO_2 treatments. At each sampling time, whole plants were harvested to determine total plant biomass. Subsequently, leaf samples were collected to quantify photosynthetic pigment contents and key sucrose metabolism indicators. Concurrently, underground rhizomes were sampled for the analysis of total saponin content. Each parameter was measured with five replicates to ensure data reliability.

2.2.2 Determination of Biomass

To determine the biomass (g/plant) of *P. japonicus* seedlings, seedlings were removed from the soil, washed to remove soil from the roots, placed in an oven at 105°C for 30 min and then dried at 70°C until a constant weight was achieved.

2.2.3 Determination of Gas Exchange Parameters

Leaf gas exchange measurements were conducted on sunny days between 9:00 and 11:00 a.m., which served as the standardized measurement window for all samples to minimize diurnal variation using a portable photosynthesis system (LICOR-6400 LI-COR Inc., USA). Within this period, measurement order of plants from different treatments and replicates was randomized to control for temporal effects. For each measurement, a fully expanded, sun-exposed leaf from the upper or middle canopy was enclosed in the standard leaf cuvette. The following cuvette conditions were maintained: the reference CO_2 concentration was dynamically controlled to match the growth condition of each plant (i.e., either 400 μmol/mol for aCO_2 chambers or the respective elevated levels for e1CO_2 and eCO_2 chambers); photosynthetic photon flux density (PPFD) was provided by the unit's built-in red-blue LED light source set to a saturating intensity of 1200 μmol/m^2/s; leaf temperature was controlled to 25°C; the vapor pressure deficit (VPD) of the air stream was maintained at 1.0 ± 0.2 kPa; and the flow rate through the cuvette was set to 500 μmol/s with the internal mixing fan operating at standard speed. The following parameters were directly recorded or calculated by the instrument's software: net photosynthetic rate (Pn), stomatal conductance (Gs), transpiration rate (Tr), and intercellular CO_2 concentration (Ci). Instantaneous water-use efficiency (WUE) was calculated

as Pn/Tr. For each treatment chamber at each time point (36 and 92 days), measurements were taken on three leaves from each of five different replicate plants, with different plants sampled at each harvest in a destructive, non-repeated measures design.

2.2.4 Determination of Photosynthetic Pigment Content

Photosynthetic pigment content was determined from fully expanded leaves sampled from the middle-upper canopy of five randomly selected plants per open-top chamber. Sampling was conducted between 9:00 and 11:00 a.m. at 36 and 92 days after the initiation of CO_2 treatments. From each plant, two leaf were excised, immediately wrapped in aluminum foil, flash-frozen in liquid nitrogen, and stored at 80°C until analysis. Approximately 0.1 g of frozen leaf tissue was finely ground in liquid nitrogen, transferred to a 15 mL centrifuge tube containing 10 mL of 95% (v/v) ethanol, and incubated in the dark at 4°C for 24 h or until the leaf tissue became colorless. The extracts were then centrifuged to remove debris. The absorbance of the supernatant was measured at 470, 649, and 664 nm using a UV-Vis spectrophotometer (UV-2600, Shimadzu, Japan) with a 1 cm path length quartz cuvette. A blank of 95% ethanol was used for baseline correction. The concentrations of chlorophyll a (Chl a), chlorophyll b (Chl b), total chlorophyll (Chl a + b), and total carotenoids (Car) were calculated using the following equations:

$$\text{Chl a } (\mu g/mL) = 13.36A_{664} - 5.19A_{649}$$

$$\text{Chl b } (\mu g/mL) = 27.43A_{649} - 8.12A_{664}$$

$$\text{Chl a + b } (\mu g/mL) = \text{Chl a} + \text{Chl b}$$

$$\text{Car } (\mu g/mL) = (1000A_{470} - 2.13 \times \text{Chl a} - 97.64 \times \text{Chl b})/209$$

Pigment contents were expressed on a fresh weight basis as micrograms per gram (mg/g FW). All extractions and measurements were performed in triplicate. Data from five plants within a chamber were averaged, and the chamber was considered the experimental unit for statistical analysis. The time from leaf harvesting to freezing did not exceed 3 min to prevent pigment degradation.

2.2.5 Determination of Sugar Content

Soluble sugar, reducing sugar, sucrose, and starch contents were quantified using colorimetric assays based on the principle of generating colored reaction products with specific reagents, followed by absorbance measurement at designated wavelengths to calculate concentrations. Soluble sugars were measured via the anthrone colorimetric method: samples were extracted with boiling water, then reacted with concentrated sulfuric acid and anthrone reagent, with absorbance read at 620 nm. Reducing sugars were determined by the 3,5-dinitrosalicylic acid (DNS) method, where alkaline heating produces a brownish-red compound measured at 540 nm. Sucrose was assayed by first removing reducing sugars via alkali treatment, followed by acid hydrolysis. The resulting glucose and fructose were quantified using the resorcinol reaction at 480 nm. Starch content was measured in samples pre-extracted with 80% ethanol to remove soluble sugars. The residue was hydrolyzed with acid to glucose, which was then quantified by the anthrone method at 620 nm. All assays employed standard curves for conversion, with final concentrations calculated based on sample mass or volume [26].

2.2.6 Determination of Enzyme Activity

Enzyme activities were measured using commercial enzyme-linked immunosorbent assay kits (Keming Biotechnology, Suzhou) following the manufacturer's protocols. SS-I (decomposing direction) activity was determined by quantifying the reducing sugars (fructose) produced from the SS-I-catalyzed reaction of sucrose with uridine diphosphate (UDP) via the DNS method at 540 nm, expressed as the amount of reducing sugars generated per gram fresh weight per unit time. SS-II (synthetic direction) activity was assessed by measuring the sucrose formation from the SS-II-catalyzed reaction of free fructose with UDPG using the sucrose-resorcinol colorimetric method at 480 nm, with activity calculated relative to a standard curve and expressed as sucrose synthesized per gram fresh weight per unit time. NI activity was determined by detecting the reducing sugars (fructose and glucose) produced from the NI-catalyzed sucrose hydrolysis via the DNS method at 510 nm, expressed as reducing sugar production per gram fresh weight per unit time. SPS activity was measured by quantifying the sucrose phosphate generated from the SPS-catalyzed reaction of fructose-6-phosphate via the resorcinol colorimetric method at 480 nm, expressed as sucrose phosphate produced per gram fresh weight per unit time. Starch phosphorylase (SP) activity was determined by monitoring the NADPH production derived from the conversion of glucose-1-phosphate, generated by the SP-catalyzed reaction of starch's α-1,4-glycosidic bonds with inorganic phosphate, through the absorbance change at 340 nm. All enzyme activity assays strictly followed the kit protocols, with reaction systems, detection wavelengths, and calculation formulas optimized for each enzyme's characteristics, and preliminary experiments conducted to ensure method reliability.

2.2.7 Determination of total Saponin Content

Total saponin content was determined using an ultrasonic extraction method followed by vanillin-perchloric acid colorimetry, with ginsenoside Re as the reference standard. Dried and powdered samples were sieved, and 0.05 g was weighed into tubes with 1 mL extraction solvent, then ultrasonically extracted for 1 h. After centrifugation at 8000× *g* and 25°C for 10 min, the supernatant was collected for analysis. For colorimetric assays, 0.5 mL supernatant was evaporated at 70°C, then mixed with 0.2 mL vanillin-acetic acid solution and 0.8 mL perchloric acid, followed by incubation in a 55°C water bath for 20 min. After adding 200 μL acetic acid to develop the color, the mixture was thoroughly vortexed, and absorbance was measured at 589 nm [27].

2.3 Statistical Analyses

Data entry and figure preparation were performed using Excel 2016 and OriginPro 2025, while statistical analyses were conducted in SPSS 23.0. The experimental unit for all analyses was the OTC. Data from plant samples (n = 5) within each chamber were averaged to obtain a single value per chamber per time point. Analysis of variance assessed the effects of CO_2 concentration (aCO_2, $e1CO_2$, $e2CO_2$), time (36/92 d) on all parameters. Residuals were checked for normality (Shapiro-Wilk) and homoscedasticity (Levene's). Post-hoc comparisons used Tukey's HSD test ($p < 0.05$). Pearson correlations were adjusted for multiple testing using the False Discovery Rate ($q < 0.05$).

3 Results

3.1 Effects of Elevated CO_2 on Biomass of P. japonicus

At 36 days, no significant differences in biomass were observed among the three CO_2 treatments. In contrast, at 92 days, the $e1CO_2$ and $e2CO_2$ treatments significantly increased the biomass by 24.45%

and 16.32%, respectively, compared to aCO_2 (Fig. 2). These results demonstrate that extended exposure to elevated CO_2, enhances plant biomass accumulation over time, with treatment effects becoming more pronounced at the later growth stage.

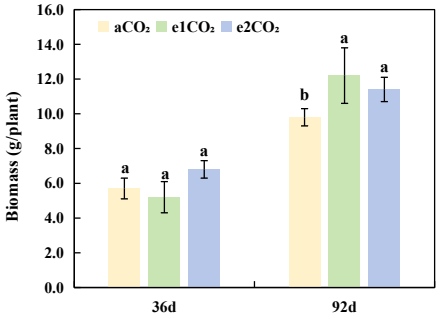

Figure 2: Effects of different treatments on biomass of *P. japonicus*. The data are expressed as the mean ± standard deviation (n = 5); Different lowercase letters for the same treatment time indicate significant differences ($p < 0.05$).

3.2 Effects of Elevated CO_2 on Gas Exchange Parameters in P. japonicus

The effects of eCO_2 on the gas exchange parameters of *P. japonicus* exhibited temporal variation during exposure (Table 1). After 36 days, both $e1CO_2$ and $e2CO_2$ treatments significantly enhanced Pn, with relative increases of 17.22% (under $e1CO_2$) and 37.78% (under $e2CO_2$) compared to aCO_2. Meanwhile, WUE increased significantly under both eCO_2 treatments, whereas Tr, Gs and Ci remained unchanged. By day 92, the responses diverged: the $e1CO_2$ treatment still markedly enhanced Pn (69.62% increase) and WUE (41.86% increase), with no detectable changes in Tr, Gs, or Ci; in contrast, the $e2CO_2$ treatment no longer exerted a significant effect on any of the measured gas exchange parameters.

Table 1: Effects of different treatments on the gas exchange parameters of *P. japonicus*.

Treatments		Pn (μmol/m²/s)	Tr (mmol/m²/s)	Gs (mo/m²/s)	Ci (μmol/m²/s)	WUE (μmol/mmol)
36 d	aCO_2	3.60 ± 0.24^{c}	3.11 ± 0.42^{a}	0.05 ± 0.01^{a}	323.57 ± 35.47^{a}	1.14 ± 0.33^{b}
	$e1CO_2$	4.22 ± 0.31^{b}	2.79 ± 0.58^{a}	0.04 ± 0.01^{a}	293.80 ± 28.39^{a}	1.50 ± 0.39^{a}
	$e2CO_2$	4.96 ± 0.29^{a}	2.96 ± 0.71^{a}	0.05 ± 0.01^{a}	329.09 ± 46.37^{a}	1.66 ± 0.51^{a}
92 d	aCO_2	4.51 ± 0.48^{b}	2.78 ± 0.76^{ab}	0.05 ± 0.03^{a}	323.91 ± 23.94^{a}	1.72 ± 0.45^{b}
	$e1CO_2$	7.65 ± 2.08^{a}	3.31 ± 0.84^{a}	0.06 ± 0.01^{a}	274.11 ± 56.50^{b}	2.44 ± 0.81^{a}
	$e2CO_2$	3.03 ± 0.73^{b}	2.24 ± 0.68^{b}	0.04 ± 0.01^{a}	324.99 ± 25.07^{a}	1.43 ± 0.41^{b}

Note: The data in the table are expressed as the mean ± standard deviation (n = 5); Different lowercase letters for the same treatment time indicate significant differences ($p < 0.05$).

3.3 Effects of Elevated CO_2 on Photosynthetic Pigment Contents of P. japonicus

After 36 days, both $e1CO_2$ and $e2CO_2$ significantly increased the contents of Chl a (by 19.20% and 24.58%, respectively) and total Chl (a + b) compared to the aCO_2 control (Table 2). Conversely, the Chl a/b was significantly reduced by 85.57% under $e2CO_2$ but was not significantly altered by $e1CO_2$ (Table 2). No significant changes were observed in Chl b or Car contents under either treatment (Table 2). Following 92 days of exposure, the $e1CO_2$ treatment sustained a significant increase in Chl a content (29.16%), with no significant effects on other pigments relative to aCO_2. In contrast, the $e2CO_2$ treatment showed no significant differences from aCO_2 for any pigment metric. Notably, at this stage, the chlorophyll a and total chlorophyll contents in the $e2CO_2$ treatment were significantly lower (by 33.95% and 29.15%, respectively) than those in the $e1CO_2$ treatment (Table 2).

Table 2: Effects of different treatments on the photosynthetic pigment content of *P. japonicus*.

Treatments		Chl a (mg/g)	Chl b (mg/g)	Chl a + b (mg/g)	Chl a/b	Car (mg/g)
36 d	aCO_2	2.97 ± 0.14^{b}	0.58 ± 0.11^{ab}	3.56 ± 0.21^{b}	5.06 ± 0.44^{b}	0.90 ± 0.13^{a}
	$e1CO_2$	3.54 ± 0.27^{a}	0.70 ± 0.15^{a}	4.24 ± 0.37^{a}	4.63 ± 0.26^{b}	1.00 ± 0.11^{a}
	$e2CO_2$	3.70 ± 0.19^{a}	0.39 ± 0.08^{b}	4.10 ± 0.14^{a}	9.39 ± 0.38^{a}	1.09 ± 0.07^{a}
92 d	aCO_2	4.63 ± 0.35^{b}	0.90 ± 0.05^{a}	5.53 ± 0.35^{ab}	5.16 ± 0.48^{a}	1.24 ± 0.31^{ab}
	$e1CO_2$	5.98 ± 0.90^{a}	1.42 ± 0.57^{a}	7.41 ± 1.47^{a}	4.51 ± 1.15^{a}	1.68 ± 0.20^{a}
	$e2CO_2$	3.95 ± 0.22^{b}	0.99 ± 0.58^{a}	4.94 ± 0.63^{b}	4.83 ± 2.12^{a}	1.08 ± 0.28^{b}

Note: The data in the table are expressed as the mean ± standard deviation (n = 5); Different lowercase letters for the same treatment time indicate significant differences ($p < 0.05$).

3.4 Effects of Elevated CO_2 on Sugar Accumulation in P. japonicus

The contents of soluble sugars and related components in *P. japonicus* under eCO_2 are presented in Fig. 3. After 36 days of treatment (Fig. 3A,C,D), the $e1CO_2$ and $e2CO_2$ treatments significantly increased the soluble sugar content by 15.57% and 35.38%, respectively, compared to aCO_2 (Fig. 3A). The sucrose and starch contents were significantly elevated only under the $e2CO_2$ treatment at this stage (Fig. 3C,D). No significant differences in reducing sugar content were detected among the treatments at 36 days (Fig. 1B). After 92 days of treatment (Fig. 3A,C,D), the $e1CO_2$ treatment significantly enhanced the contents of soluble sugars, sucrose, and starch by 34.10%, 39.19%, and 36.74%, respectively, relative to aCO_2. In contrast, the $e2CO_2$ treatment significantly increased sucrose content by 16.68% but had no significant effect on soluble sugar or starch contents (Fig. 3A,C,D). The reducing sugar content remained unaffected by any CO_2 treatment at 92 days (Fig. 3B). Furthermore, compared to the $e1CO_2$ treatment, the $e2CO_2$ treatment led to significantly lower levels of soluble sugars, sucrose, and starch at 92 days (Fig. 3A,C,D).

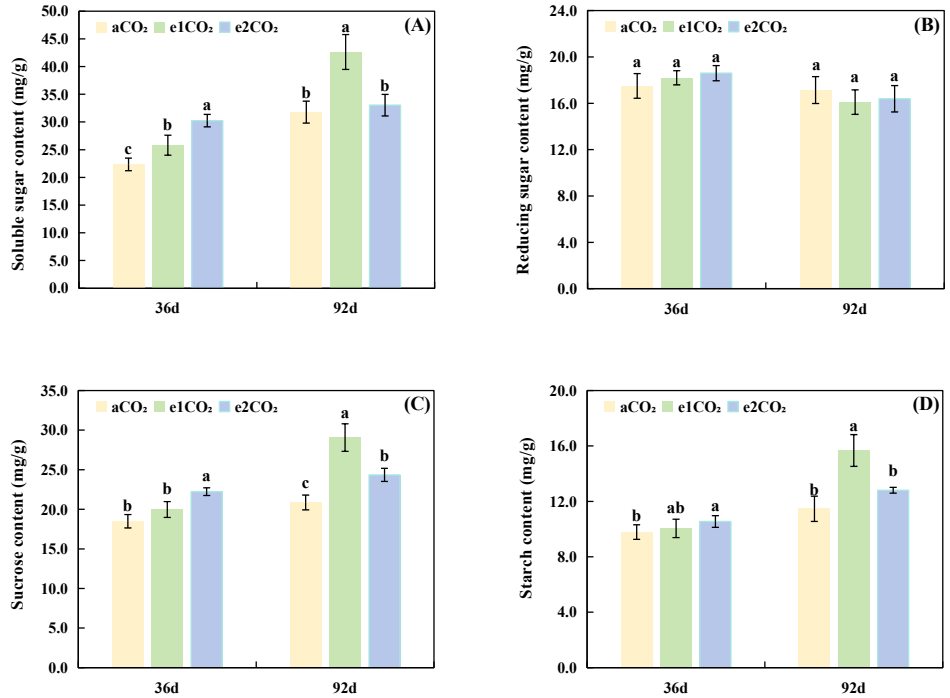

Figure 3: Effects of different treatments on soluble sugar accumulation in *P. japonicus*. The data are expressed as the mean ± standard deviation (n = 5); Different lowercase letters for the same treatment time indicate significant differences ($p < 0.05$). (**A**) Soluble sugar content. (**B**) Reducing sugar content. (**C**) Sucrose content. (**D**) Starch content.

3.5 Effects of Elevated CO_2 on Sucrose Metabolism-Related Enzyme Activities in P. japonicus

The activities of key sucrose metabolism enzymes are shown in Fig. 2. At the 36-day time point (Fig. 4A–E), eCO_2 significantly affected several enzymes. The activities of SS-II (Fig. 4B) and SPS (Fig. 4E) were significantly enhanced by eCO_2. In contrast, the activities of SS-I (Fig. 4A) and NI (Fig. 4C) were significantly reduced. The activity of SP (Fig. 4D) was not significantly altered. At the 92-day time point (Fig. 4A–E), the responses differed between CO_2 levels. The $e1CO_2$ treatment significantly decreased SS-I activity (by 19.35%) but significantly increased the activities of SS-II (by 4.72%), NI (by 50.82%), SP (by 22.20%), and SPS (by 72.99%) compared to aCO_2. The $e2CO_2$ treatment significantly elevated SPS activity by 11.78% relative to aCO_2 but showed no significant effects on the activities of SS-I, SS-II, or SP.

3.6 Effects of Elevated CO_2 on Total Saponin Content in P. japonicus

As shown in Fig. 5, after 36 days of treatment, elevated CO_2 concentrations ($e1CO_2$ and $e2CO_2$) had no significant effect on total saponin content in the rhizomes of *P. japonicus* compared to the aCO_2 control. After 92 days of treatment, both $e1CO_2$ and $e2CO_2$ treatments significantly increased total saponin content in the rhizomes, with $e1CO_2$ and $e2CO_2$ treatments showing 15.16% and 10.98% increases, respectively, compared to the aCO_2 control. No significant difference in total saponin content was observed between the $e1CO_2$ and $e2CO_2$ treatments.

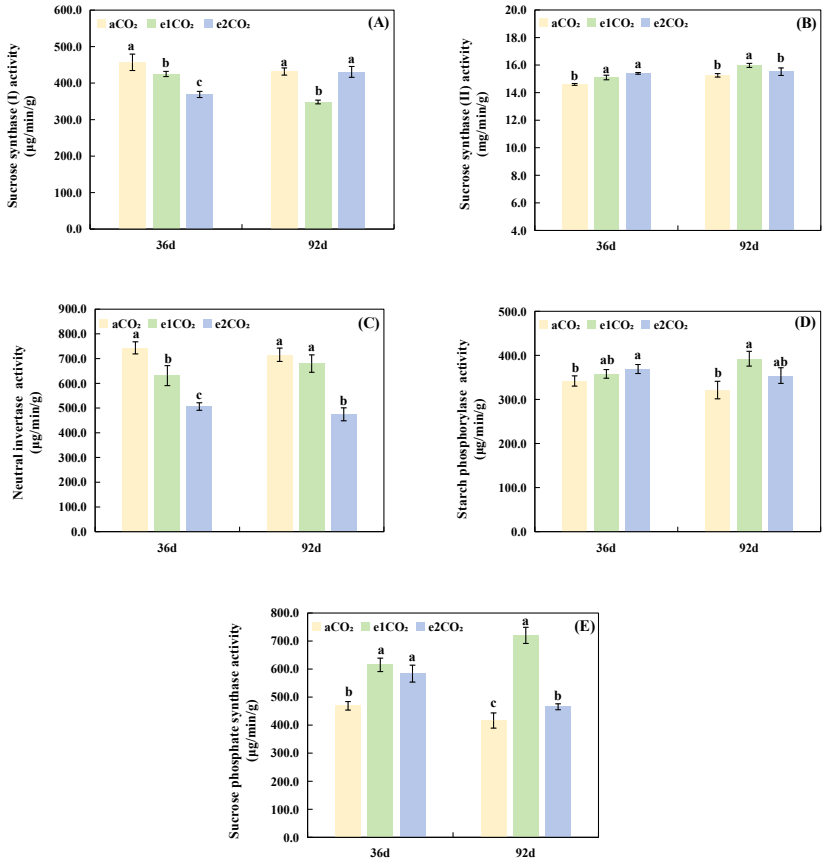

Figure 4: Effects of different treatments on the activities of enzymes related to sucrose metabolism in *P. japonicus*. The data are expressed as the mean ± standard deviation (n = 5); Different lowercase letters for the same treatment time indicate significant differences ($p < 0.05$). (**A**) Sucrose synthase (I) activity. (**B**) Sucrose synthase (II) activity. (**C**) Neutral invertase activity. (**D**) Starch phosphorylase activity. (**E**) Sucrose phosphate synthase activity.

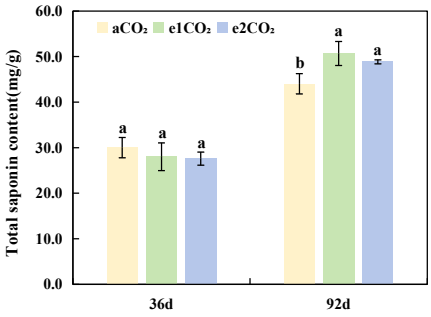

Figure 5: Effects of different treatments on total saponin content in *P. japonicus*. The data are expressed as the mean ± standard deviation (n = 5); Different lowercase letters for the same treatment time indicate significant differences ($p < 0.05$).

3.7 Correlation Analysis

Correlation analysis between leaf sucrose metabolism indicators and rhizome total saponin content in *P. japonicus* revealed significant positive correlations between rhizome total saponin content and leaf soluble sugar content, sucrose content, starch content, and SS-II activity (Fig. 5). No significant correlations were observed between rhizome total saponin content and SS-I, NI, SP activity, or SPS activity (Fig. 6).

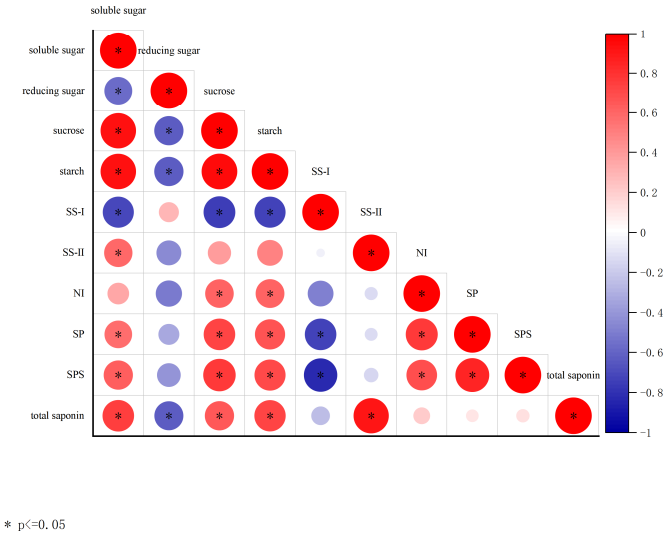

Figure 6: Correlation analysis. Color intensity represents correlation strength, with red indicating positive correlations and blue indicating negative correlations. $^{*}p \leq 0.05$.

4 Discussion

The effect of eCO_2 on plant photosynthetic characteristics depends not only on the concentration but also on the exposure duration, as CO_2 serves as the primary substrate for photosynthesis [28]. While short-term eCO_2 exposure often promotes growth, its effects can diminish over time due to feedback mechanisms such as carbohydrate accumulation and carbon-nitrogen imbalance [29]. In this study, short-term eCO_2 significantly enhanced Pn and chlorophyll content in *P. japonicus*. However, as the treatment progressed, the two elevated CO_2 levels ($e1CO_2$, $e2CO_2$) showed clearly divergent temporal patterns: the moderate elevation ($e1CO_2$) sustained a measurable, though gradually dampened, photosynthetic stimulation, whereas the stimulatory effect of the high concentration ($e2CO_2$) on Pn and

chlorophyll content was transient, becoming statistically indistinguishable from aCO_2 in the later growth stage (Tables 1 and 2). This difference indicates that the magnitude of CO_2 elevation is a critical factor in determining how rapidly photosynthetic down-regulation occurs. The more rapid and pronounced accumulation of carbohydrates under $e2CO_2$ likely triggered stronger and earlier feedback inhibition, potentially via sugar-signaling pathways and/or an accelerated progression into sink limitation or nitrogen dilution [29,30]. Consequently, although both eCO_2 treatments increased final biomass relative to aCO_2, the weaker biomass gain under $e2CO_2$ compared with $e1CO_2$ at 92 days corresponds with its earlier and more complete loss of photosynthetic advantage. These findings align with reports in crops such as soybean [31] and the medicinal plant *Polygonatum kingianum* [4], and underscore the well-documented interaction between CO_2 concentration and exposure time in plant responses to eCO_2 [32,33]. Together, they demonstrate that the effects of eCO_2 are dynamic rather than static, and that predicting CO_2-driven growth and metabolic responses requires considering both concentration and duration as interacting variables, with particular attention to the transient nature of the photosynthetic stimulation under high-level, long-term eCO_2.

Our results demonstrate a clear temporal dissociation between the initial stimulation of carbon metabolism and the eventual accumulation of saponins in *P. japonicus* under eCO_2, a phenomenon consistent with known plant resource allocation strategies [30]. At 36 days, both $e1CO_2$ and $e2CO_2$ treatments significantly enhanced the net photosynthetic rate (by 17.22% and 37.78%, respectively; Table 1), soluble sugar content (by 15.57% and 35.38%; Fig. 3A), and the activities of key sucrose-metabolizing enzymes, including SS-II and SPS, compared to aCO_2 (Fig. 4B,E). This initial boost in photosynthesis and carbohydrate metabolism is a typical plant response to eCO_2 [32]. Despite this pronounced upregulation in photosynthetic capacity and carbohydrate availability, the total saponin content in the rhizomes remained unchanged at this early stage (Fig. 5). This suggests a prioritization of photoassimilates towards primary metabolic processes and structural growth [34], reflecting source-sink dynamics where carbon is preferentially allocated to biomass accumulation during the initial vegetative growth phase, thereby delaying significant investment into secondary metabolite biosynthesis. By 92 days, the physiological responses diverged. The $e1CO_2$ treatment sustained its promotional effects, resulting in a 15.16% increase in total saponin content over aCO_2 (Fig. 5). In contrast, while the $e2CO_2$ treatment also increased saponin content relative to aCO_2, its level was significantly lower than that under $e1CO_2$ (Fig. 5). The eventual saponin accumulation under $e1CO_2$ can be attributed to a sustained surplus of carbon fixation over the longer term, which, after meeting the demands of primary growth, provided ample substrates for secondary metabolism [35]. The correlation analysis provides a mechanistic clue: saponin content exhibited a significant positive correlation with SS-II activity (Fig. 6) but not with SPS activity. This indicates that the SS-catalyzed reaction, which produces UDPG–a direct glycosyl donor for glycosyltransferases [18]—may play a more critical role in directing carbon toward saponin accumulation than does SPS, a pattern observed in other saponin-producing species. We acknowledge that the absence of leaf nitrogen data limits a definitive mechanistic understanding of the attenuated response under prolonged $e2CO_2$, which we hypothesize may involve a carbon-nitrogen imbalance, a common constraint under high CO_2 conditions [36]. Furthermore, while total triterpenoid saponins are a key quality metric [10], the lack of individual ginsenoside profiling means shifts in the composition of specific bioactive compounds remain unexplored.

The differential outcomes at 92 days highlight the critical role of above-ground physiology—modulated by CO_2 concentration—in determining the medicinal quality of below-ground organs [3]. The superior saponin accumulation under $e1CO_2$ aligns with the sustained upregulation of photosynthetic parameters and sucrose metabolism enzymes observed throughout the experiment. The finding that rhizome saponin

content was significantly associated with leaf sucrose content, leaf starch content, and SS-II activity (Fig. 6) strongly supports a model where eCO_2-enhanced carbon assimilation in leaves fuels the production and translocation of sucrose to underground sinks [19,37]. The positive association with SS activity is consistent with the established pathway where sucrose cleavage by SS provides UDPG for the glycosylation of triterpenoid aglycones, a critical final step in saponin biosynthesis [18,35]. Therefore, the increased saponin yield under $e1CO_2$ can be interpreted as a direct consequence of a prolonged and balanced enhancement of the source (leaf photosynthesis and sucrose synthesis) and sink (rhizome) strength, facilitating the channeling of carbon precursors into the saponin biosynthetic pathway [38] (Fig. 7). In contrast, the weaker promotion of photosynthesis and sucrose metabolism by $e2CO_2$ at 92 days, suggests a potential constraint, possibly at the metabolic or nutrient level. The observed pattern is consistent with the hypothesis of a developing imbalance in carbon and nitrogen metabolism under long-term, highly elevated CO_2, which can lead to photosynthetic acclimation and disrupt optimal resource allocation to secondary metabolites [36,39]. This interpretation is cautious, as it is based on physiological responses without direct nitrogen data. Similar context-dependent effects of eCO_2 duration and concentration on secondary metabolism have been reported in other medicinal plants, underscoring the complexity of these interactions [40]. Collectively, our findings demonstrate that the effect of eCO_2 on saponin accumulation is not linear but depends critically on both the concentration and of exposure duration, mediated through its integrated effects on source activity and carbon partitioning.

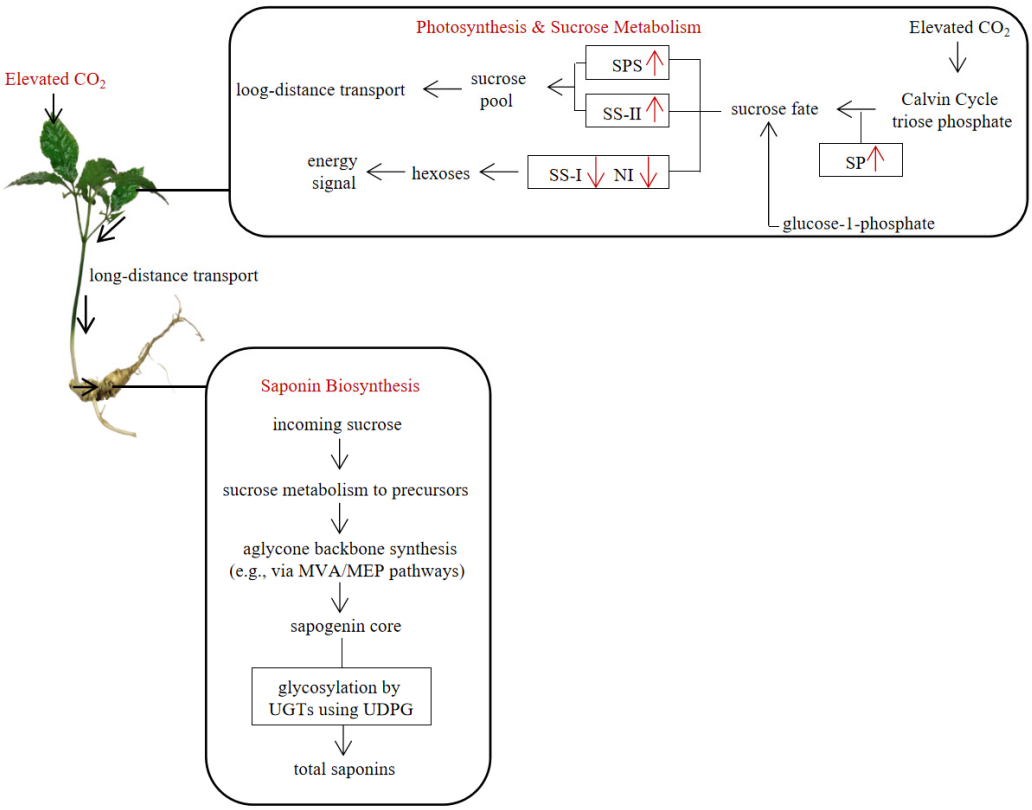

Figure 7: The interrelationship among leaf photosynthesis, sugar metabolism, and rhizome saponin biosynthesis in *P. japonicus.* An upward-pointing red arrow (↑) indicates an increase in the activity of the corresponding enzyme, a downward-pointing red arrow (↓) indicates a decrease in the activity of the corresponding enzyme.

5 Conclusions

In summary, a moderate elevation of CO_2 significantly enhanced the total saponin content in *P. japonicus* rhizomes by sustainably improving the net photosynthetic rate and upregulating key sugar-metabolizing enzyme activities, thereby facilitating carbon assimilation and translocation to sink organs. However, a higher CO_2 concentration led to diminished promotional effects over time, likely due to feedback inhibition from excessive carbohydrate accumulation. These findings suggest the potential of CO_2 management as an agronomic strategy for quality improvement of this medicinal plant under future climate scenarios; from an agronomic perspective, they imply that cultivating *P. japonicus* under controlled or moderately eCO_2 levels could be employed to optimize saponin yield and consistency, provided that excessive carbohydrate buildup is avoided through appropriate canopy management, balanced fertilization (especially N input to match altered C:N ratios), and timely harvesting before feedback inhibition reduces efficacy. Meanwhile, irrigation scheduling may be refined to exploit the increased water-use efficiency associated with eCO_2, further supporting stable growth and secondary metabolite production. This highlighting the need for future studies to focus on elucidating the associated molecular mechanisms—particularly the expression of genes involved in sucrose-to-saponin biosynthesis—and to evaluate the response of individual saponin components for a comprehensive quality assessment, and on validating these cultivation strategies under multi-factor field conditions to ensure their practical applicability in future climates.

Acknowledgement: Not applicable.

Funding Statement: This research was funded by the Guizhou Province Technology Plan Project, Qiankehe Basic-ZK [2023] General 023, Key 002 and Guizhou Province Project for the Growth of Young Scientific and Technological Talents in General Higher Education Institutions, QianJiao He Foundation, Grant No. (2022)029.

Author Contributions: Study conception and design: Xiao Wang; data collection: Deyan Li; analysis and interpretation of results: E Liang, Xiaohui Song; draft manuscript preparation: Xiao Wang. All authors reviewed and approved the final version of the manuscript.

Availability of Data and Materials: The authors confirm that the data supporting the findings of this study are available within the article.

Ethics Approval: Not applicable.

Conflicts of Interest: The authors declare no conflicts of interest.

References

1. World Meteorological Organization (WMO). The State of Greenhouse Gases in the Atmosphere Based on Global Observations through 2022 [Internet]. 2023 [cited 2025 Nov 1]. Available from: https://wmo.int/publication-series/wmo-greenhouse-gas-bulletin-no-19.
2. Kimball BA. Crop responses to elevated CO_2 and interactions with H_2O, N, and temperature. Curr Opin Plant Biol. 2016;31:36–43. [CrossRef].
3. Gamage D, Thompson M, Sutherland M, Hirotsu N, Makino A, Seneweera S. New insights into the cellular mechanisms of plant growth at elevated atmospheric carbon dioxide concentrations. Plant Cell Environ. 2018;41(6):1233–46. [CrossRef].
4. Zhao M, Jia H, Zhao J, Wang Y, Laraib I, Shi X, et al. Response of cultivation suitability for *Polygonatum kingianum* to climate change in China. Environ Earth Sci. 2025;84(11):285. [CrossRef]
5. Yang HM, Li LP, Sun M, Chen HY, Li LY, Feng CH. Response of leaf hydraulic traits of *Typha orientalis* to simulated warming and elevated CO_2 concentration. Bull Bot Res. 2023;43(5):729–40.

6. Liang Z, Luo Z, Li W, Yang M, Wang L, Lin X, et al. Elevated CO_2 enhanced the antioxidant activity and downregulated cell wall metabolism of wolfberry (*Lycium barbarum* L.). Antioxidants. 2021;11(1):16. [CrossRef].
7. He M, Zhang J, Wang Z, Li J, Ye G, Ye Q. Effects of doubling the CO_2 concentration on photosynthetic characteristics and growth of *Dendrobium officinale*. Guangdong Agric Sci. 2020;47(2):17–23. [CrossRef].
8. Al Jaouni S, Saleh AM, Wadaan MA, Hozzein WN, Selim S, AbdElgawad H. Elevated CO_2 induces a global metabolic change in basil (*Ocimum basilicum* L.) and peppermint (*Mentha piperita* L.) and improves their biological activity. J Plant Physiol. 2018;224:121–31. [CrossRef]
9. Qiang Q, Gao Y, Yu B, Wang M, Ni W, Li S, et al. Elevated CO_2 enhances growth and differentially affects saponin content in *Paris polyphylla* var. yunnanensis. Ind Crop Prod. 2020;147:112–24. [CrossRef]
10. Chen Y, Liu M, Wen J, Yang Z, Li G, Cao Y, et al. *Panax japonicus* CA Meyer: a comprehensive review on botany, phytochemistry, pharmacology, pharmacokinetics and authentication. Chin Med. 2023;18(1):148. [CrossRef]
11. Chan HH, Sun HD, Reddy MVB, Wu TS. Potent α-glucosidase inhibitors from the roots of *Panax japonicus* CA Meyer var. major. Phytochemistry. 2010;71(11–12):1360–64. [CrossRef]
12. Wang XJ, Xie Q, Liu Y, Jiang S, Li W, Li B, et al. *Panax japonicus* and chikusetsusaponins: a review of diverse biological activities and pharmacology mechanism. Chin Herb Med. 2020;13(1):64–77. [CrossRef].
13. Du Z, Li J, Zhang X, Pei J, Huang L. An integrated LC-MS-based strategy for the quality assessment and discrimination of three *Panax* species. Molecules. 2018;23(11):2988. [CrossRef]
14. Rai A, Yamazaki M, Takahashi H, Nakamura M, Kojoma M, Suzuki H, et al. RNA-seq transcriptome analysis of *Panax japonicus*, and its comparison with other *Panax* species to identify potential genes involved in the saponins biosynthesis. Front Plant Sci. 2016;7:481. [CrossRef].
15. Yao L, Lu J, Wang J, Gao WY. Advances in biosynthesis of triterpenoid saponins in medicinal plants. Chin J Nat Med. 2020;18(6):417–24. [CrossRef].
16. Börnke F, Sonnewald S. Biosynthesis and metabolism of starch and sugars. In: Plant metabolism biotechnol. Hoboken, NJ, USA: John Wiley & Sons, Inc.; 2011. p. 1–25. [CrossRef].
17. Wittich PE, Willemse MTM. Sucrose utilization during ovule and seed development of *Gasteria verrucosa* (Mill.) H. Duval as monitored by sucrose synthase and invertase localization. Protoplasma. 1999;208(1):136–48. [CrossRef].
18. Zhao J, Wang R, Zhao S, Wang Z. Advance in glycosyltransferases, the important bioparts for production of diversified ginsenosides. Chin J Nat Med. 2020;18(9):643–58. [CrossRef].
19. Hou M, Wang R, Zhao S, Wang Z. Ginsenosides in *Panax* genus and their biosynthesis. Acta Pharm Sin B. 2021;11(7):1813–34. [CrossRef].
20. Jang IB, Lee DY, Yu J, Park HW, Mo HS, Park KC, et al. Photosynthesis rates, growth, and ginsenoside contents of 2-yr-old *Panax ginseng* grown at different light transmission rates in a greenhouse. J Ginseng Res. 2015;39(4):345–53. [CrossRef].
21. Hao L, Liu Y, Dong G, Liu J, Qiu K, Li X, et al. Multi-strategy ugt mining, modification and glycosyl donor synthesis facilitate the production of triterpenoid saponins. Front Plant Sci. 2025;16:1586295. [CrossRef].
22. Zhang H, Li G, Zhao C, Zhao P, Jiang M, Wen G, et al. Characterizations of "drumstick-forming" on saponin contents of Notoginseng *Radix* et Rhizoma and their saccharide metabolism basis of vegetative organs of *Panax notoginseng*. Ind Crops Prod. 2022;180:114699. [CrossRef].
23. Qaderi MM, Martel AB, Strugnell CA. Environmental factors regulate plant secondary metabolites. Plants. 2023;12(3):447. [CrossRef]
24. Zhou J, Xu Z, Yu Z, Mai H, Huang J, Chang X, et al. Growth, development and reproduction of meadow moth *Loxostege sticticalis* fed on pea seedlings grown under elevated CO_2. Agronomy. 2024;15(1):30. [CrossRef]
25. IPCC. Climate Change 2021: the physical science basis. In: Contribution of working group I to the sixth assessment report of the intergovernmental panel on climate change. Cambridge, UK: Cambridge University Press; 2021. p. 1–13. [CrossRef].
26. Maness N. Extraction and analysis of soluble carbohydrates. Methods Mol Biol. 2010;639:341–70. [CrossRef].
27. Mursaliyeva VK, Sarsenbek BT, Dzhakibaeva GT, Mukhanov TM, Mammadov R. Total content of saponins, phenols and flavonoids and antioxidant and antimicrobial activity of *in vitro* culture of *Allochrusa gypsophiloides* (Regel) Schischk compared to wild plants. Plants. 2023;12(20):3521. [CrossRef]
28. Woodward FI. Potential impacts of global elevated CO_2 concentrations on plants. Curr Opin Plant Biol. 2002;5(3):207–11. [CrossRef].

29. Moore BD, Cheng SH, Sims D, Seemann JR. The biochemical and molecular basis for photosynthetic acclimation to elevated atmospheric CO_2. Plant Cell Environ. 1999;22(6):567–82. [CrossRef].
30. Su YX, Zhao P, Jia LJ, Cao YF, Liu GZ, Chen JW, et al. Deep application of controlled-release urea increases the yield and saponin content of *Panax notoginseng* by regulating soil nitrate distribution. Front Plant Sci. 2025;15:1505702. [CrossRef].
31. Kaur R, Durstock M, Prior SA, Runion GB, Ainsworth EA, Baxter I, et al. Investigating the impact of elevated CO_2 on biomass accumulation and mineral concentration in foliar and edible tissues in soybeans. Plant Cell Environ. 2025;48(12):8712–26. [CrossRef].
32. Ainsworth EA, Long SP. 30 years of free-air carbon dioxide enrichment (FACE): what have we learned about future crop productivity and its potential for adaptation? Glob Chang Biol. 2021;27(1):27–49. [CrossRef].
33. Poorter H, Knopf O, Wright IJ, Temme AA, Hogewoning SW, Graf A, et al. A meta-analysis of responses of C_3 plants to atmospheric CO_2: dose-response curves for 85 traits ranging from the molecular to the whole-plant level. New Phytol. 2022;233(4):1560–96. [CrossRef].
34. Darko E, Heydarizadeh P, Schoefs B, Sabzalian MR. Photosynthesis under artificial light: the shift in primary and secondary metabolism. Philos Trans R Soc Lond B Biol Sci. 2014;369(1640):20130243. [CrossRef].
35. Zhang HL. Study on mechanism of high saponin contents of Notoginseng Radix et Rhizoma characterized by "Drumstick-forming" [dissertation]. Kunming, China: Yunnan University; 2022. [CrossRef].
36. Ainsworth EA, Long SP. What have we learned from 15 years of free-air CO_2 enrichment (FACE)? A meta-analytic review of the responses of photosynthesis, canopy properties and plant production to rising CO_2. New Phytol. 2005;165(2):351–71. [CrossRef].
37. Jiang N, Jin LF, Teixeira da Silva JA, Islam MZ, Gao HW, Liu YZ, et al. Activities of enzymes directly related with sucrose and citric acid metabolism in *Citrus* fruit in response to soil plastic film mulch. Sci Hortic. 2014;168:73–80. [CrossRef].
38. Ghasemzadeh A, Jaafar HZE. Effect of CO_2 enrichment on synthesis of some primary and secondary metabolites in ginger (*Zingiber officinale* Roscoe). Int J Mol Sci. 2011;12(2):1101–14. [CrossRef].
39. Hamilton JG, Zangerl AR, DeLucia EH, Berenbaum MR. The carbon–nutrient balance hypothesis: its rise and fall. Ecol Lett. 2001;4(1):86–95. [CrossRef].
40. Idso S, Kimball B. Effects of long-term atmospheric CO_2 enrichment on the growth and fruit production of sour orange trees. Glob Change Biol. 1997;3(2):89–96. [CrossRef].